Clin Oral Invest (2012) 16:489–498
DOI 10.1007/s00784-011-0525-z

ORIGINAL ARTICLE

Fracture toughness of dental restorative materials

Nicoleta Ilie · Reinhard Hickel · Anca Silvia Valceanu · Karin Christine Huth

Received: 14 October 2010 / Accepted: 14 February 2011 /

Abstract The ability of a restorative material to withstand fracture is of crucial importance especially in stress-bearing area. Therefore, the study aims to analyse the fracture toughness of a large number of dental restorative materials categories. The fracture toughness (K_{IC}) of 69 restorative materials belonging to ten materials categories—micro-hybrid, nanofilled, microfilled, packable, ormocer-based, and flowable resin-based composites (RBC), compomers and flowable compomers, as well as glass ionomer cements (GIC) and resin-modified GIC was measured by means of the single-edge notched-beam method after storing the samples ($n=8$) for 24 h in distilled water. Data were analyzed with the one-way analysis of variance (ANOVA) followed by the Tukey's test and partial eta-squared statistics ($p<0.05$). Large variations between the tested materials within a material category were found. The lowest fracture toughness was reached in the GIC group, followed by the microfilled RBCs, resin-modified GIC, and flowable compomers, which do not differ significantly among each other as a material group. The ormocer-based, packable, and micro-hybrid RBCs performed statistically similar, reaching the highest fracture toughness values. Between the two categories of flowables—composites and compomers—no differences were measured. The correlation between K_{IC} and filler volume (0.34) and respective filler weight (0.40) was low. K_{IC} increased with the volume fraction of fillers until a critical value of 57%, following with a plateau, with constant values until ca. 65% volume fraction. Above this value, K_{IC} decreased slightly. Due to the very large variability of the fracture toughness within a material type, the selection of a suitable restorative material should have not been done with respect to a specific material category, especially in stress-bearing areas, but by considering the individual measured material properties.

Keywords Fracture toughness · Composites · Mechanical properties

Introduction

Whereas, the most common reason for failure in restorations with posterior resin composites were long time attributed above all to secondary caries [1], evidence from newer surveys of prospective studies indicate bulk fracture in composite fillings as the most common cause for restoration replacement after 5 years [2]. Fracture of restoration was also shown to be the primary reason for failure in composite restoration placed in larger cavities for periods longer than 11 years [3, 4].

A valuable and intensively used tool to characterize the fracture resistance of materials is the measurement of fracture toughness, describing an intrinsic characteristic of a material to resist fracture, or the amount of stress that is required to propagate through a pre-existing flaw [5, 6]. The study of fracture toughness is based on the theoretical

N. Ilie (✉) · R. Hickel · K. C. Huth
Department of Restorative Dentistry,
Dental School of the Ludwig-Maximilians-University,
Goethestr. 70,
Munich 80336, Germany
e-mail: nicoleta.ilie@dent.med.uni-muenchen.de

A. S. Valceanu
Department of Dento-Facial Aesthetics,
Dental School of the Victor Babes University,
P-ta Eftimie Murgu, No. 2,
Timisoara, Romania
e-mail: asvalceanu@yahoo.com

considerations of Griffith [5] made initially for brittle materials and modified later by Irwin [6] to explain the crack growth also in ductile materials. Griffith considered that a low fracture resistance of a material is due to the presence of microscopic flaws in the bulk material and demonstrated empirically that the product of the square root of the flaw length (a) and the stress at fracture (σ_f) was nearly constant ($\sigma_f\sqrt{a} = \text{constant} = C$). He further observed that the growth of a crack requires the creation of two new surfaces, hence an increase in surface energy, and found that the constant he previously specified is proportional to the Young's modulus (E) and the surface energy of the material (γ), [5] being described by the equation $C = \sqrt{\frac{2E\gamma}{\pi}}$.

In later research, Irwin realized that plasticity must also play an important role in the fracture of ductile materials, since a plastic zone develops at the tip of the crack, increasing in size as the applied load increases. The plastic loading and unloading cycle near the crack tip leads to the dissipation of energy in form of heat, making it necessary to introduce a dissipative term [6] to the energy balance relation described by Griffith for brittle materials. This means that additional energy is needed for crack growth in ductile materials when compared to brittle materials. Irwin divided the energy needed for crack growth into two parts: the stored elastic strain energy which is released as a crack grows (like in brittle material) and the dissipated energy which includes plastic dissipation and the surface energy. The dissipated energy provides the thermodynamic resistance to fracture [6].

Griffith's energy criterion: $\sigma_f\sqrt{a} = C = \sqrt{\frac{2E\gamma}{\pi}}$ was modified by Irwin in $\sigma_f\sqrt{a} = \sqrt{\frac{EG}{\pi}}$ with $G=2\gamma$ for brittle materials [6].

Irwin also found that the stress field around a sharp crack in a linear elastic material could be defined by a parameter which he termed as the stress intensity factor, K [6]. He stated that fracture occurs when the value of K exceeds a critical value, K_c. Thus, K is a stress field parameter independent of the material, whereas K_c is often referred as the fracture toughness, and is a measure of an inherent material property. For the specific case of plane strain deformation, K_c becomes K_{Ic}, with the subscript I defining the different ways of loading a material to enable a crack to propagate (mode I=crack opening under a normal tensile stress perpendicular to the crack).

Numerous test techniques for measuring fracture toughness are available, albeit no standard specimen type is defined. These methods include double torsion, indentation crack length/fracture, indentation strength, Chevron notch bend specimen, double cantilever beam, single-edge notched beam (SENB), single-edge pre-cracked beam, fractography approach, or compression pre-cracking [7–10]. The most common used method to determine the fracture toughness of dental materials is the single-edge notch test and the short rod Chevron notch test on cylindrical, rectangular, and prismatic specimens [11].

Our study aimed to compare 69 frequently used restorative materials belonging to ten material categories—micro-hybrid, nanofilled, microfilled, packable, ormocer-based, flowable composites, compomers and flowable compomers, as well as glass ionomer cements (GIC) and resin-modified GIC—in terms of their fracture toughness, determined by the SENB method. Several other mechanical properties of the above mentioned materials, measured under identical storage and curing conditions, have already been published in large part previously [12] and served as a reference.

The null hypothesis tested was that there are no differences in fracture toughness among the ten material categories.

Materials and methods

The 69 restorative materials comprising 10 materials categories—micro-hybrid, nanofilled, microfilled, packable, ormocer-based and flowable composites, compomers and flowable compomers, as well as GIC and resin-modified GIC—are described in Table 1.

The *fracture toughness* (K_{Ic}) was determined according to ASTM designation E 399-83 [13], using eight single-edge notched-beam specimens of each material. The specimens (16 mm length×2 mm height×2 mm width) were made by compressing the restorative material between two glass plates with intermediate polyacetate sheets, separated by a steel mould. Irradiation occurred on top and bottom of the specimens for 40 s in a light curing oven (Dentacolor XS, Kulzer, Wehrheim, Germany), which assured that the whole surface was cured at the same time. After removal from the mould, the specimens were ground with silicon carbide sand paper [grit size P 1200/4000 (Leco)] in order to get rid of disturbing edges or bulges. All specimens were then stored in distilled water at 37°C prior to testing for 24 h. A notch (0.3 mm wide, 1 mm deep) was then machined for each specimen with a diamond saw (Proxxon, Hermann, Tonisvorst, Germany) using water coolant. The width of the notch was determined by the thickness of the blade, whereas the standardization of the notch's depth was assured by a sliding mechanism installed on the saw and adjusted to stop the intrusion of the blade at 1-mm distance from the sample's surface. The depth of the notch was measured with a microscope (component part of the Fischerscope H100C, Helmut-Fischer GmbH, Sindelfingen-Maichingen, Germany) and varied between 0.90 and 1.10 mm. The

Table 1 Materials, manufacturer, chemical composition of the matrix and filler and filler content by weight and volume percent

Material	Manufacturer/batch	Resin matrix	Filler	Content wt/vol
Hybrid RBCs				
Adamant Cavifil	Vivadent/E 52179	BisGMA, UDMA, TEGMA	Ba-glass, YbF_3, SiO_2, MO	81/62
Arabesk Top	VOCO/94816	BisGMA, UDMA, TEGDMA	Glass ceramic	77/56
Ariston pHc	Vivadent/B21705	BisGMA, UDMA, TEGDMA	Alkaline glass, Ba-Al-F-Si-glass, YbF_3, SiO_2	79/59
Beautifil	Shofu/050143	BisGMA, TEGDMA	F-B-Al-Si-glass	83.3/68.6
Brillant	Coltene/IA350	BisGMA, BisEMA, TEGDMA	B-glass, SiO_2	78/59
CapoCom.4	GDF/P 9.42	BisGMA, UDMA, TEGDMA	Glass, Pyrog. SiO2	80/NI
Charisma	Heraeus Kulzer/10023	BisGMA, TEGDMA	Ba-Al-F-glass, SiO_2	78/61
Clearfil ST	Kuraray/00002A	BisGMA, TEGDMA	Ba-glass, SiO_2	86/70
Ecusit® composite	DMG/99260036	BisGMA, UDDMA, TEDMA	Ba-glass, pyrogen SiO_2	77/57
Enamel plus HFO	GDF/2000002388	BisGMA, UDMA, TEGMA	Glass filler, SiO_2	75/53
Esthet X	Dentsply/0112121	BisGMA, BisEMA, TEGDMA	Ba-F-Al-B-Si-glass, SiO_2	77/60
Herculite XRV	Kerr/909065	BisGMA, TEGDMA	Al-B-Si-glass, SiO_2	79/59
Filtek Silorane (Hermes)	3M ESPE/A-094	3,4-Epoxycyclohexylethylcyclo-polymethylsiloxane Bis-3, 4-epoxycyclohexylethyl-phenylmethylsilane	Silanized quartz, YF	76/55
InTenS	Vivadent/RZB 033	BisGMA, UDMA, BisEMA	Ba-glass,YbF_3, copolymers	74/51
Miris	Coltene/KI272	Methacrylate	Ba-glass, SiO_2 glass	80/65
Pertac II	3M-ESPE/025	Bifunctional methacrylates	Quartz, SiO_2,YF_3	80/61
Point 4	Kerr/102A48	BisGMA, TEGDMA	Ba-Al-B-Si-glass, SiO_2	76/57.2
Prodigy	Kerr/812898	BisGMA, TEGDMA, EBADM, UV-9	Ba-Al-Zn-oxide, SiO_2	79/59
Superlux Universalhybrid	DMG/991600018	BisGMA, UDMA, TEGDMA, HDDMA	Ba-glass, pyrogen SiO_2, Al-silicate, polymer powder	83/75
Synergy Duo Shade	Coltene/IG079	BisGMA, BisEMA, TEGDMA	Sr-glass, Ba-glass, SiO_2	74/59
Tetric	Vivadent/C16884	BisGMA; UDMA, TEGDMA	Ba-glass, YbF_3, SiO_2, MO	81/62
Tetric Ceram	Ivoclar-Vivadent D00037	BisGMA, UDMA, TEGDMA	Ba-glass, Ba-Al-F-Si-glass, YbF_3, SiO_2, MO	78.6/60
TPH Spectrum™	Dentsply/9907000556	BisGMA, BisEMA, TEGDMA	Ba-Al-B-Si-glass, SiO_2	77/57
Venus	Heraeus Kulzer/010022	BisGMA, TEGDMA	SiO_2, Ba-Al-B-F-Si -Glass	79/61
Z100	3M ESPE/2EG	BisGMA, TEGMA	ZrO_2/SiO_2	84.5/64.2
Z250	3M ESPE/20011016	BisGMA, UDMA, BisEMA	ZrO_2/SiO_2	84.5/60
Nano RBCs				
Filtek Supreme	3M ESPE RBX/2003	BisGMA, BisEMA, UDMA, TEGDMA	ZrO_2/SiO_2 cluster SiO_2 nanofiller	78.5/59.5
Microfilled composite				
Durafill	Heraeus Kulzer/121	BisGMA, TEGDMA, UDMA	SiO_2, splitter polymerisate	60/40
Heliomolar radiopaque	Ivoclar-Vivadent D03569	BisGMA, UDMA, DDMA	YbF_3, SiO_2 77,8 wt-gesamt%	66.7/46
Silux Plus™	3M 9EY/19990630	BisGMA, TEGDMA	SiO_2, Prepolym.	56/40

Table 1 (continued)

Material	Manufacturer/batch	Resin matrix	Filler	Content wt/vol
Packable RBCs				
Alert	Jeneric/Pentron 840971	PCDMA, UDMA	Ba-B-Al-Si-glas, SiO_2, Glasfiber	81/67
Filtek P60	3M ESPE	BisGMA, BisEMA,UDMA	ZrO_2/SiO_2	83/61
Prodigy Condensable	Kerr/812898	BisGMA, TEGDMA	SiO_2, Ba-Al-B-Si-glass	80/61.7
Solitaire 1	Heraeus Kulzer/42	Multi-acrylate monomers	Porous SiO_2 glass Ba–Al–F–Si glass	65/NI
Solitaire 2	Heraeus Kulzer 020224	UDMA, BisGMA, TEGDMA, TFM	Porous SiO_2, Ba-Al-B-F-Si glass	75/58
Surefil	Dentsply/020307	UDMA	Ba-F-Al-B-Si-glas, SiO_2-glass	82/66
Synergy Compact	Coltene/IH405	BisGMA, BisEMA, UDMA	Sr-glass, Ba-glass, SiO_2	74/59
Tetric Ceram Condensable	Ivoclar-Vivadent RZ-A025	BisGMA, UDMA, DDM	Ba-glass, Ba-Al-F-Si-glass, YbF_3, SiO_2, MO	81/63
Ormocer-based Composites				
Definite	Degussa/1985201	Ormocere®, Polysiloxan, Bis-EMA, DDM	Ba-glass, Aerosile, modified Apatit	77/61
Admira	VOCO/94512	Ormocere®, BisGMA, UDMA, TEGDMA, BHT	SiO_2, Ba-Al-B-Si-glass	77.0/60.2
Compomeres				
Compoglass F	Ivoclar-Vivadent 900507	UDMA, TEGDMA cycloaliphatic dicarboxylic acid dimethacrylate	YbF_3, Ba-Al-F-Si-glass, MO	77/55
Dyract	Dentsply 9909000736	UDMA, TCB	Sr-Al-Na-F-P-Si-glass; SrF_2	72/49
Dyract AP	Dentsply 9909000819	UDMA, TCB, APM	Sr-Al-Na-F-P-Si-glass; SrF_2	75/53
Elan	Kerr/901201	Polycarboxylic acid, UDMA, TEGDMA	Ba-Al-B-silicate, Na-F-silicate, SiO_2	–
F2000 Rasant	3m 9BR/19990817	Polycarboxylic acid, GDMA, polyvinylpyrrolidone;	F-Al-silicate glass	84/67
Glasiosite	VOCO 92538	BisGMA, diUDMA, TEGDMA, BHT	Glass ceramics, silicates	77.5/NI
Hytac	ESPE FW0050451	Co-monomers	YF_3, SiO_2, (Ca, Zn)FAlSi-glass	66/–
Luxat	DMG 99270049	Monomers	Anorganic filler	–
GIC				
Ionofil Molar AC	VOCO, 06078	Polyacrylic acid, tartaric acid	Silicate glass	–
Ketac Fil	ESPE, 0054/0014			–
Ketac Silver	ESPE, 0078			–
Ketac Molar	ESPE, 0100/0015	Copolymer from acrylic and maleic acid	Al-Ca-La-F-Si-glass	–
Hi Dense	Shofu Dental GmbH, 060016-1			–
Fuji IX	GC, 0004043	Polyacrylic acid	Al-Si-glass	–

Resin-modified GIC				
Vitremer	3M, 20000307	Modified polyalkenoic acid	F-Al-Si-glass	–
Photac Fil	ESPE, FW0066256	Polyalkenoic acid, 2-hydroxyethylmethacrylat	F-Al-Si-glass	–
Fuji II LC	GC, 0003211	Polyacrylic acid, 2-hydroxyethylmethacrylat, UDMA	Al-Si-glass	–
Flowable RBCs				
Admira Flow	VOCO/99791	Ormocere®, Methacrylate, BHT	Inorganic filler	64/50.5
Arabesk Flow	Voco/91658	BisGMA, UDMA, TEGDMA	SiO_2,Ba-Sr-B-silicate	64.0/50.3
Definite Flow	Degussa 3004400	Ormocere®, Polysiloxan, Bis-EMA, DDM	Ba-glass, Aerosile, modified Apatit	63/–
FLOWline	Heraeus Kulzer 80021	Methacrylates, TEGDMA	Iorganic filler	62/41
Palfique Estelite High Flow	Tokuyama/106	BisGMA, TEGDMA	SiO_2-ZrO_2, SiO_2-TiO_2	68/50
Palfique Estelite Low Flow	Tokuyama/506	BisGMA, TEGDMA	SiO_2-ZrO_2, SiO_2-TiO_2	65/50
Reference Flow	ESPE 643902001	BisGMA	Inorganic filler	
Revolution	Kerr 9-1294	BisGMA	Inorganic filler	–
Tetric Flow	Ivoclar-Vivadent J12549	BisGMA, UDMA, TEGDMA	Ba-glass, YbF_3, Ba-Al-F-Si-glass, SiO_2, MO	68.1/43.8
Flowable compomers				
Compoglass Flow	Ivoclar-Vivadent A03341	UDMA, TEGDMA cycloaliphatic dicarboxylic acid dimethacrylate	YbF_3, Ba-Al-F-Si glass, MO	66.8/41.8
Dyract Flow	Dentsply 10800023	Ammonium salt of PENTA and N,N-dimethyl aminoethyl methacrylate, carboxylic acid modified methacrylates, DGDMA	Sr-Al-Na-F-P-Si-glass, SiO_2	59/43
PrimaFlow	DMG/99260209	UDMA, acidic methacrylates	Ionomer Glas, SiO_2	64/40

Data are provided by manufacturers

BisGMA bisphenol-A diglycidyl ether dimethacrylate, *BisEMA* bisphenol A polyetheylene glycol diether dimethacrylate, *TEGDMA* triethylene glycol dimethacrylate, *UDMA* urethane dimethacrylate, *DMDMA* decamethylendimethacrylate, *DGDMA* diethylene glycol dimethacrylate, *DGDMA* diethylene glycol dimethacrylate, *IBMA* isobornylmethacrylate, *PENTA* dipentaerythritol penta acrylate monophosphate, *TCB* resin tetracarboxylic acid-hydroxyethylmethacrylate-ester, *HPMA* 3-hydroxpropyl methacrylate, *ETMAL* ethyltriglycol methacrylate, *APM* alkanoyl-poly-methacrylate, *DM* dimethacrylate resin, *MS* methacrylate modified polysiloxane, *DDMA* decandioldimethacrylate, *TFM* tetrafunctionalmonomers, *DDM* decandiol dimethacrylate, *MO* mixed oxide, *PPF* prepolymerised Filler.

samples were loaded until failure in an universal testing machine (MCE 2000ST, quick test Prüfpartner GmbH, Langenfeld, Germany) in a three-point bending test device, which is constructed according to the guidelines of NIST No. 4877 (Span=S=12 mm) [14]. During testing, the specimens were immersed in distilled water at room temperature. The crosshead speed was 0.5 mm/min. The universal testing machine measured the force during bending as function of deflection of the beam. Load-deflection (P=load) curves were recorded; the height (B) and the width (W) of the specimens were measured with a micrometer and the notch depth (a) with a measuring microscope. K_{IC} was calculated from measurements with the single-edge notched-beam specimens as [15, 16]:

$$K_{IC} = \frac{3(a/W)^{1/2}\left[1.99 - a/W(1 - a/W)(2.15 - 3.93a/W + 2.7(a/W)^2\right]PS}{2(1 + 2a/W)(1 - a/W)^{3/2}BW^{3/2}}$$

Results were statistically compared within each material category as well as among the material categories using one-way ANOVA and Tukey HSD post hoc test (α=0.05). A multivariate analysis (general linear model) tested the influence of the parameters filler volume and weight as well as material category on the measured properties (SPSS Inc.; Chicago, IL, USA, version 17.0).

Results

The results of the measurements are summarized in Tables 2 and 3 and Fig. 1.

Large variations between the tested materials within a material category were found. Post hoc multiple pairwise comparisons with Tukey's HSD test ($p<0.05$) (Table 2) showed that, within the tested material categories, the lowest fracture toughness was reached in the GIC group, followed by the microfilled resin-based composites (RBCs), resin-modified GIC, and flowable compomers, which do not differ significantly among each other as a material group. The ormocer-based, packable, and micro-hybrid RBCs performed statistically similar reaching the highest fracture toughness values. Between the two categories of flowables—composites and compomers—no differences were measured.

The influence of the parameters "filler volume", "filler weight", and "material category" as well as their interaction products were analyzed in an ANOVA multivariate test. The fracture toughness was selected as dependent variables. The significance values of these three main effects were less than 0.05, indicating that they contribute all to the model. The results of the ANOVA multivariate test are summarized in Table 3, showing that the strongest influence on the mechanical properties (higher eta square values) was performed by the filler weight, followed by filler volume and material category. The influence of all three parameter was very high.

An excellent linear correlation was found between filler volume and filler weight (0.93), whereas the correlation between K_{IC} and filler volume (0.34) and respective filler weight (0.40) was rather low.

Figure 1 presents the variation of the K_{IC} as function of filler volume and weight for all materials, without considering their belonging to a material group. An Epanechnikov kernel function [9] was used for contouring the areal density of the measured data, showing an increase in K_{IC} with the volume fraction of fillers until a critical volume fraction of 57%, following with a plateau, with constant values until ca. 65%. Above this value, K_{IC} decrease slightly. As for the variation of K_{IC} with the filler weight, a straight increase until a filler weight of 78% was observed, with a further constant K_{IC} as the filler weight increases.

Discussion

The SENB method used to determine the fracture toughness in this study has been commonly used in other research, primarily because of its simplicity [7]. The sharp crack requirement is replaced by a narrow notch, which is easy to introduce and can be measured more accurately. Fracture toughness measurements using a single-edge notched-beam are usually conducted by means of a three- or four-point bending apparatus, both methods being widely used in dental material research, thus allowing to operate the experiment at low equipment expenses. But it has also been reported that the results of this test are very sensitive to the notch width and depth [7], making a direct comparison of different studies difficult. The present study allows, thus to distinguish explicitly between the facture behaviour of a large number of restorative materials, since the sample preparation and measuring conditions were identical.

The majority of studies are in general agreement that the fracture toughness of composites increases as filler volume fraction is increased [9]. In general, it was shown that

Table 2 Fracture toughness, mean, and standard deviation

	K_{IC} [MPa√m]
Hybrid RBCs	
Beautifil	0.97^{a} (0.25)
CapoCom.4	1.03^{a} (0.15)
Venus	1.18^{abc} (0.21)
Superlux Universalhybrid	1.59^{bcd} (0.13)
Filtek Silorane (Hermes)	1.64^{bcde} (0.21)
Tetric Ceram	1.70^{cde} (0.18)
Brillant	1.74^{de} (0.34)
Z100	1.81^{def} (0.22)
Clearfil ST	1.81^{def} (0.44)
Pertac II	1.86^{def} (0.48)
Charisma	1.87^{defg} (0.20)
InTenS	1.87^{defg} (0.31)
Point 4	1.89^{defg} (0.40)
Ariston pHc	1.92^{defg} (0.19)
Herculite XRV	1.96^{defg} (0.25)
Prodigy	1.98^{defg} (0.22)
Tetric	2.00^{defg} (0.18)
Arabesk Top	2.01^{defg} (0.16)
TPH Spectrum	2.09^{defg} (0.22)
Synergy Duo Shade	2.12^{efg} (0.21)
Ecusit Composite	2.13^{efg} (0.21)
Esthet X	2.15^{efg} (0.25)
Miris	2.17^{efg} (0.33)
Z250	2.31^{fg} (0.16)
Enamel plus	2.40^{g} (0.56)
Adamant Cavifil	2.40^{g} (0.42)
Nano RBCs	K_{IC} [MPa√m]
Filtek Supreme	1.46 (2.28)
Microfilled RBCs	K_{IC} [MPa√m]
Durafill	0.83^{a} (0.09)
Silux Plus	0.96^{a} (0.13)
Heliomolar radiopaque	1.27^{b} (0.15)
Packable RBCs	K_{IC} [MPa√m]
Solitaire 1	1.37^{a} (0.17)
Tetric Condensable	1.55^{ab} (0.43)
Prodigy Condensable	1.56^{ab} (0.35)
Synergy Compact	1.61^{ab} (0.20)
Surefil	1.69^{ab} (0.44)
Solitaire 2	1.86^{bc} (0.13)
P60	2.20^{c} (0.17)
Alert	2.27^{c} (0.17)
Ormocer-based Composites	K_{IC} [MPa√m]
Admira	1.58^{a} (0.31)
Definite	1.67^{a} (0.19)
Compomeres	K_{IC} [MPa√m]
Elan	0.77^{a} (0.16)
F2000 Rasant	0.78^{a} (0.08)
Dyract AP	1.44^{b} (0.35)
Dyract	1.46^{b} (0.17)
Glasiosite	1.54^{b} (0.07)
Compoglass F	1.69^{bc} (0.17)
Hytac	1.86^{cd} (0.18)
Luxat	1.98^{d} (0.11)
GIC	K_{IC} [MPa√m]
Ionofil Molar AC	0.37^{a} (0.09)
Ketac Fil	0.39^{a} (0.08)
Ketac Silver	0.44^{a} (0.08)
Ketac Molar	0.48^{a} (0.13)
Hi Dense	0.52^{a} (0.19)
Fuji IX	0.53^{a} (0.09)
Resin-modified-GIC	K_{IC} [MPa√m]
Vitremer	0.87^{a} (0.24)
Fuji II	1.16^{ab} (0.34)
Photac Fil	1.32^{bc} (0.26)
Flowable RBCs	FS [MPa]
Admira Flow	0.96^{a} (0.24)
Palfique Estelite Low Flow	1.12^{ab} (0.33)
FLOWline	1.37^{bc} (0.18)
Reference Flow	1.40^{bc} (0.18)
Definite Flow	1.41^{bc} (0.28)
Revolution	1.46^{bc} (0.20)
Palfique Estelite High Flow	1.60^{c} (0.32)
Tetric Flow	1.68^{c} (0.16)
Arabesk Flow	1.68^{c} (0.20)
Flowable Compomers	
Dyract Flow	0.98^{a} (0.18)
PrimaFlow	1.16^{a} (0.10)
Compoglass Flow	1.74^{b} (0.21)
Material Type	K_{IC} [MPa√m]
GIC	0.45^{a} (0.12)
Microfilled RBCs	1.02^{b} (0.22)

Table 2 (continued)

	K_{IC} [MPa√m]
Resin-modified-GIC	1.12^{bc} (0.33)
Flowable compomers	1.29^{bcd} (0.37)
Flowable RBCs	1.41^{cde} (0.32)
Compomers	1.44^{cde} (0.46)
Nano RBCs	1.46^{cde} (0.28)
Ormocer-based Composites	1.55^{def} (0.27)
Packable RBCs	1.77^{ef} (0.41)
Hybrid RBCs	1.84^{f} (0.45)

Data are arranged in ascending order of the mean fracture toughness value

Superscript letters indicate statistically homogeneous subgroups (Tukey's HSD test, α=0.05)

fracture toughness was highest in the more heavily filled resins being also independent of degree of conversion in the matrix [17]. The presence of reinforcing particles distributes the propagating nominal force into many components, causes the crack front to curve or dissipate between particles, and becomes energetically unfavourable for a crack to grow. Within the tested RBCs in this study, however a low correlation between K_{Ic} and filler volume was measured (0.34) suggesting a more complicated dependency between materials structure and K_{Ic} as well as different origins for flaws in the measured materials. Fracture origins in filled resins were shown to be manifold, including particle agglomerates associated with problems in mixing, wetting, or in the distribution of the filler phases in the composite [10], air bubbles, resin rich areas, poorly bonded particles, or even the filler particles themselves if they are larger than 100 μm or the particles are inherently weak [10].

Our study showed that K_{IC} increased with the volume fraction of fillers only until a critical volume fraction of 57%, following with a plateau, with constant values until ca. 65%. Above this value, K_{IC} decrease slightly probably due to an increased concentration of flaws—voids, porosities, and filler agglomerates—being incorporated in the material as a consequence of an increase in viscosity (Fig. 1). The GIC and resin-modified GIC were not included in this calculations, since the role of the fillers in this materials is not primarily to enforce the material but to contribute to the hardening process of the cements and thus the filler dimension will change in time.

Table 3 Influence of fillers—volume vol. percent and weight wt. percent—and material type on fracture toughness expressed by partial eta-squared statistics

Variables	Vol. %	Wt. %	Material type
Fracture toughness	0.463	0.485	0.455

The fracture toughness measured in our study correlates significantly with the flexural strength (0.7), flexural modulus (0.6), diametral tensile strength (0.5), and compressive strength (0.4) determined for the same materials under identical storage and curing conditions [12].

Besides the matrix-filler interaction, crack pinning, crack branching, crack deflection, or micro crack-induced toughening are seen as main mechanisms of increasing fracture toughness values by filler particles in resin composites [17–19]. The mechanism of increasing toughness by matrix-filler interaction seems to play an important function especially in RBCs with decreased filler size, like the nano-hybrid materials. For the fracture toughness analysis in this study, we have chosen the first commercial available nano RBCs (Filtek Supreme). Whereas nano-hybrid RBCs contain besides nano-filler also larger bulk fillers are the fillers in the nano RBC Filtek Supreme a combination of non-aggregated nano-filler, and loosely bound agglomerated nano-clusters. The decreased filler size is able to change the organic matrix between the particles, improving the mechanical properties, as a consequence of decreasing interparticle distances. This so-called interfacial region is responsible for communication between the matrix and filler and is conventionally ascribed properties different from the bulk matrix because of its proximity to the surface of the filler [20]. It was also shown that nano-particles create local properties in RBCs, with a spatial distribution of the nano-dynamic-mechanical properties, suggesting a graduated structure, with a smooth transition from the stiff filler to the softer matrix [21]. On the other hand, nano-filled composites containing ultra-small filler particles enlarged the filler surfaces relative to the volume size, resulting in a larger interface between filler and organic matrix, and thus a higher susceptibility to hydrolytically degradation and a faster degradation of mechanical properties, when compared to micro-hybrid RBCs [22]. These contradictory properties are also reflected in the measured behaviour of nano-hybrid RBCs in different studies. Using a similar method to determine the fracture toughness as in our test, Lin and Drummond [23] analysed three direct dental composites—a micro-filled (Micronew), a micro-hybrid (Renew), and a nano-filled (Filtek Supreme Plus)—and an indirect dental composite (BelleGlass HP), with non-aged samples as control versus 5-month aging in air, distilled water, artificial saliva, and a 50/50 mixture of water and ethanol. No differences in fracture toughness were found in the non-aged samples between the micro- and nano-hybrid materials, both performing better than the micro-filled RBC and worse than the indirect dental composite. Aged Filtek Supreme Plus however, showed increased failure

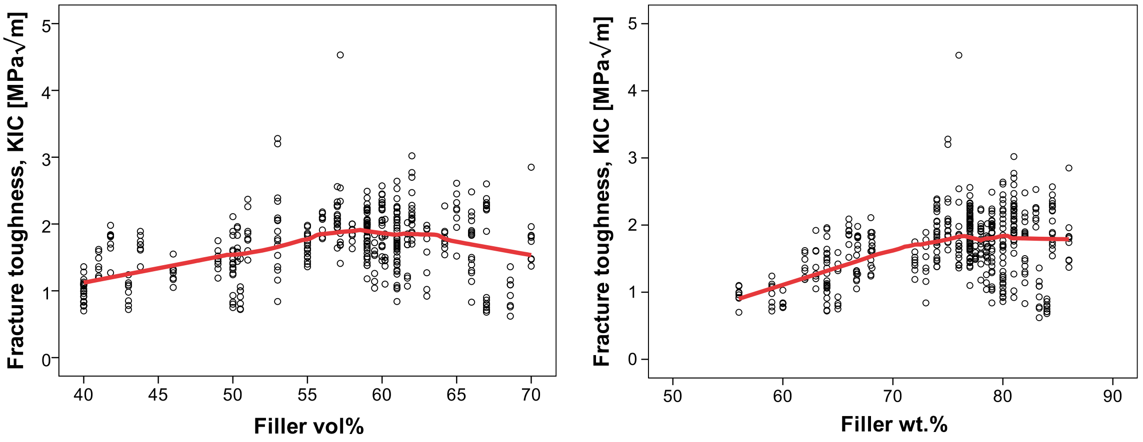

Fig. 1 Fracture toughness as function of filler volume and weight

during cyclic fatigue loading and a significantly decreased fracture toughness, when compared to the micro-hybrid material [23]. These results stay in contrast to other observations showing that the nano-clusters in Filtek Supreme Plus provide a distinct fracture mechanisms in the composite [24], resulting in significant improvements in strength and reliability when subjected to cyclic pre-loading [25], predicting an improvement in fatigue and thus an enhanced clinical longevity of the material. The discrepancies between the abovementioned studies are mainly due to differences in environmental storage and testing conditions, since the first study used a 5-month aging and the last one only 24 h. Also other studies showed that RBCs experience a significant reduction (from 30% to 56%) in K_{Ic} after being aged (75% ethanol for 6 months). Since a similar reduction in K_{Ic} of 58% was measured also for the unfilled resin, the authors attributed the reduction of K_{Ic} in composites to a weakening of the resin matrix, which facilitated crack propagation [26].

The lowest fracture toughness values were measured for the class of glass ionomer cements. Despite presenting numerous outstanding characteristics as a restorative material, being the only restorative material capable of forming stable physicochemical bonds to both enamel and dentin [27], with a good biocompatibility, resistance to microleakage [28] as well as a low coefficient of thermal expansion [29], glass ionomer cements are brittle and have poor mechanical properties, thus limiting their clinical use as a permanent filling material in the posterior region [28, 29].

To improve the mechanical properties, resin-modified glass ionomer cements and polyacid-modified composite resins (compomers) were developed, having an additional light polymerization which substantiates the chemical hardening process in the initial critical phase in GIC [30, 31]. Within the measured materials in this study, there were no significant differences between the resin modified-GIC and the compomers, both showing significantly higher fracture toughness compared to GIC, being comparable with the microfilled, flowables, and nano-hybrid RBCs. Compared to the micro-hybrid RBCs, the class of compomers showed significantly lower fracture toughness as a material category, being in agreement with previous studies [18]. Yap at al. comparing three compomer—Compoglass F, F2000, Dyract Posterior—and three composite—Tetric Ceram, Z250, Esthet-X restoratives (single-edged notched specimens (25×2×2 mm), storage: 1 week in distilled water at 37°C) showed that the fracture toughness in compomers (0.97–1.23 MPam$^{1/2}$) was significantly lower than in composites (1.75–1.92 MPam$^{1/2}$). The poorer resistance to crack propagation in compomers (lower fracture toughness) when compared to the micro-hybrid RBCs correlates also with the filler content, being lower in compomers [12], as well as with other mechanical properties, since it was shown that compomers also exhibit a significant lower flexural strength than micro-hybrid RBCs [12].

The fracture toughness of the two measured ormocer-based RBCs proved to be high, being comparable to the micro-hybrid and packable RBCs. Both materials contain besides ormocers also traditional monomers (Table 1). However, Janda et al. [32] showed that compared to non-aged conditions (water storage for 24 h at 37°C), the flexural strength of Admira decreased after aging (30-day water storage at 37°C, followed by 5,000 thermocycles between +5°C and +55°C) even under the 80 MPa limit of ISO 4049 for occlusal fillings, whereas the flexural strength of Definite did not changed significantly.

The high-viscosity packable RBCs showed excellent fracture toughness values, being however comparable to the micro-hybrid and the ormocer-based RBCs. This material category was developed in an attempt to increase the mechanical properties of RBC restorations in stress-bearing areas, to limit wear and fracture of the restoration within the body and at the margins, and to reduce the polymerization shrinkage. It was shown that materials with higher filler contents exhibited a tendency towards improved fatigue resistance. Lohbauer et al. measured for the packable RBC Surefil the best results under cyclic fatigue conditions, albeit all materials tested, including micro-hybrid RBCs were proved to suffer from a decrease in strength due to mechanical fatigue within 10,000 cycles [33].

Conclusion

The ability of a restorative material to withstand fracture was shown to be dependent by the material category; therefore, our working hypothesis must be rejected.

The data proved a very large variability of the fracture toughness within a material category; consequently, the selection of a suitable restorative material especially in stress-bearing areas should not been done with respect to a specific material category but by considering the measured material properties. The micro-hybrid RBCs proved to have comparable fracture toughness as the packable and ormocer-based RBCs and were superior in their ability to withstand fracture to all other material categories, including the measured nano-hybrid material. An increase of fracture toughness with the filler volume was observed only until a filler level of 57%.

Conflict of interest The authors declare that they have no conflict of interest.

References

1. Sarrett DC (2005) Clinical challenges and the relevance of materials testing for posterior composite restorations. Dent Mater 21:9–20
2. Brunthaler A, Konig F, Lucas T, Sperr W, Schedle A (2003) Longevity of direct resin composite restorations in posterior teeth. Clin Oral Investig 7:63–70
3. van Dijken JW (2000) Direct resin composite inlays/onlays: an 11 year follow-up. J Dent 28:299–306
4. Van Nieuwenhuysen JP, D'Hoore W, Carvalho J, Qvist V (2003) Long-term evaluation of extensive restorations in permanent teeth. J Dent 31:395–405
5. Griffith AA (1921) The phenomena of rupture and flow in solids. Philos Trans R Soc Lond 221:163–198
6. Irwin G (1957) Analysis of stresses and strains near the end of a crack traversing a plate. J Appl Mech 24:361–364
7. Schneider SJ (1991) Engineered materials handbook. ASM International, USA
8. Fujishima A, Ferracane JL (1996) Comparison of four modes of fracture toughness testing for dental composites. Dent Mater 12:38–43
9. Kovarik RE, Fairhurst CW (1993) Effect of Griffith precracks on measurement of composite fracture toughness. Dent Mater 9:222–228
10. Quinn JB, Quinn GD (2010) Material properties and fractography of an indirect dental resin composite. Dent Mater 26:589–599
11. Soderholm KJ (2010) Review of the fracture toughness approach. Dent Mater 26:e63–e77
12. Ilie N, Hickel R (2009) Investigations on mechanical behaviour of dental composites. Clin Oral Investig 13:427–438
13. ASTM-Standard-E399-83 (1989) Standard Test Method for Plane Strain Fracture Toughness of Metallic Materials American Society for Testing and Materials Annual Book of ASTM Standards, Philadelphia, PA
14. Quinn GD (1992) Room-temperature flexure fixture for advanced ceramics. NISTIR 4877 National Institute of Standards and Technology, Gaithersburg, MD
15. Srawley JE, Brown WF (1964) Fracture toughness testing methods. Fracture Toughness Testing and Its Applications ASTM Special Publ:133–196
16. De Groot R, Van Elst HC, Peters MCRB (1988) Fracture mechanics parameters for failure prediction of composite resins. J Dent Res 67:919–924
17. Ferracane JL, Antonio RC, Matsumoto H (1987) Variables affecting the fracture toughness of dental composites. J Dent Res 66:1140–1145
18. Yap AU, Chung SM, Chow WS, Tsai KT, Lim CT (2004) Fracture resistance of compomer and composite restoratives. Oper Dent 29:29–34
19. Kim KH, Park JH, Imai Y, Kishi T (1994) Microfracture mechanisms of dental resin composites containing spherically-shaped filler particles. J Dent Res 73:499–504
20. Wagner D, Vaia R (2004) Nanocomposites: issues at the interface. Materials Today 7(11):38–42
21. Ilie N, Hickel R, Watts DC (2009) Spatial and cure-time distribution of dynamic-mechanical properties of a dimethacrylate nano-composite. Dent Mater 25:411–418
22. Ilie N, Hickel R (2009) Macro-, micro- and nano-mechanical investigations on silorane and methacrylate-based composites. Dent Mater 25:810–819
23. Lin L, Drummond JL (2010) Cyclic loading of notched dental composite specimens. Dent Mater 26:207–214
24. Curtis AR, Palin WM, Fleming GJ, Shortall AC, Marquis PM (2009) The mechanical properties of nanofilled resin-based composites: characterizing discrete filler particles and agglomerates using a micromanipulation technique. Dent Mater 25:180–187
25. Curtis AR, Palin WM, Fleming GJ, Shortall AC, Marquis PM (2009) The mechanical properties of nanofilled resin-based composites: the impact of dry and wet cyclic pre-loading on bi-axial flexure strength. Dent Mater 25:188–197
26. Ferracane JL, Berge HX (1995) Fracture toughness of experimental dental composites aged in ethanol. J Dent Res 74:1418–1423
27. Glasspoole EA, Erickson RL, Davidson CL (2002) Effect of surface treatments on the bond strength of glass ionomers to enamel. Dent Mater 18:454–462
28. Mount GJ (1994) Buonocore memorial lecture. Glass-ionomer cements: past, present and future. Oper Dent 19:82–90
29. Naasan MA, Watson TF (1998) Conventional glass ionomers as posterior restorations. A status report for the American Journal of Dentistry. Am J Dent 11:36–45
30. Burgess J, Norling B, Summitt J (1994) Resin ionomer restorative materials: the new generation. J Esthet Dent 6:207–215
31. Sidhu SK, Watson TF (1995) Resin-modified glass ionomer materials. A status report for the American Journal of Dentistry. Am J Dent 8:59–67
32. Janda R, Roulet JF, Latta M, Ruttermann S (2006) The effects of thermocycling on the flexural strength and flexural modulus of modern resin-based filling materials. Dent Mater 22:1103–1108
33. Lohbauer U, von der Horst T, Frankenberger R, Kramer N, Petschelt A (2003) Flexural fatigue behavior of resin composite dental restoratives. Dent Mater 19:435–440